0038-075X/07/17201-27–41
Soil Science

January 2007
Vol. 172, No. 1
Printed in U.S.A.

# NITRATE MOBILITY UNDER UNSATURATED FLOW CONDITIONS IN FOUR INITIALLY DRY SOILS

Barry J. Allred[1], Glenn O. Brown[2], and Jerry M. Bigham[3]

**Solving environmental problems associated with nitrate ($NO_3^-$) requires a better understanding of how $NO_3^-$ moves through the soil profile. Transient unsaturated horizontal column experiments were conducted to assess processes affecting soil $NO_3^-$ transport. Duplicate tests were conducted on four soils having different physicochemical and mineralogical properties. In each test, a 200 mg/L $NO_3^-$-nitrogen ($NO_3^-$-N) solution was applied at the inlet of the relatively dry soil columns, and the value of sorptivity kept constant at 0.0073 cm/sec$^{0.5}$. Comparison of corresponding soil water content and soil solution $NO_3^-$-N concentration profiles from the column tests clearly indicated anion exclusion to be an important process impacting $NO_3^-$ mobility under unsaturated flow conditions. Evidence of anion exclusion for all four soils included soil solution $NO_3^-$-N concentrations near the inlet that were 13% to 21% less than the concentration (200 mg/L $NO_3^-$-N) injected at the inlet. Further evidence of anion exclusion included peak soil solution $NO_3^-$-N concentrations up to twice the injected concentration near the wetting front for three of the four soils. The fourth soil, possibly because of a combination of dispersion processes, low pH, and the mixture of clay minerals present, behaved somewhat differently than the other soils by having a peak soil solution $NO_3^-$-N concentration above 200 mg/L located approximately halfway between the column inlet and wetting front. Overall, this research indicated that anion exclusion can be a key process affecting $NO_3^-$ mobility in a variety of soil environments. (Soil Science 2007;172:27–41)**

**Key words: Nitrate mobility, unsaturated flow, soil properties, anion exclusion, anion adsorption.**

NITRATE ($NO_3^-$) is the most widespread contaminant found in ground water (Freeze and Cherry, 1979). In particular, inorganic/organic fertilizer applications on farm fields are commonly responsible for $NO_3^-$ contamination in shallow aquifers (Nolan and Stoner, 2000). Investigations conducted by the US Geological Survey have found that 20% of the shallow wells sampled in agricultural areas exceeded the US Environmental Protection Agency drinking water standard of 10 mg/L $NO_3^-$-N (US Geological Survey, 2001). Nitrogen discharged by the Mississippi River has resulted in the spring/summer formation of a hypoxic zone near the US coast in the Gulf of Mexico (Goolsby and Battaglin, 2000), where oxygen concentrations of less than 2 mg/L cause stress or death in bottom-dwelling organisms. Midwest agriculture is a large source of the nitrogen (N) producing the Gulf of Mexico hypoxic zone, because the Midwest contains the greatest amount of subsurface drainage infrastructure of any region in the United States (US Department of Agriculture, Economic Research Service, 1987). Nitrate-nitrogen from fertilizer applied to Midwest farm fields is discharged into local waterways via these subsurface drainage systems at concentrations often approaching

[1]Soil Drainage Research Unit, US Department of Agriculture Agricultural Research Service, Room 234, 590 Woody Hayes Drive, Columbus, OH 43210. Dr. Allred is corresponding author. E-mail: allred.13@osu.edu

[2]Biosystems and Agricultural Engineering Department, Oklahoma State University, Stillwater, OK.

[3]School of Natural Resources, Ohio State University, Columbus, OH.

Received Apr. 17, 2006; accepted Aug. 28, 2006.

DOI: 10.1097/01.ss.0000240548.44551.74

50 mg/L (Zucker and Brown, 1998). For most of the $NO_3^-$ involved with aquifer contamination and hypoxic zone environmental problems, initial transport is through the soil profile. Solving these environmental problems will require, at least partly, a better understanding of the processes affecting soil profile $NO_3^-$ mobility under unsaturated flow conditions.

Nitrate mobility in the soil environment is governed largely by electrostatic interactions between negatively charged $NO_3^-$ ions and either soil minerals or soil organic matter. Electrostatic adsorption, or anion adsorption, occurs when $NO_3^-$ ions become attached to positively charged exchange sites on a soil surface. A significant percentage of exchange sites on soil mineral and organic matter are pH dependent. Under low pH conditions, positively charged hydrogen ions ($H^+$) become attached to certain exchange site functional groups, thereby causing these exchange sites to become positively charged (Bohn et al., 1985; Foth, 1984).

Kaolinite, a layered aluminosilicate mineral, allophane, an amorphous aluminosilicate mineral, and various iron/aluminum oxides/hydroxides are all examples of minerals that may develop a net positive surface charge given a sufficiently low pH environment (Gustafsson, 2001; Sposito, 1984). The point of zero charge (PZC) is the pH value of a soil solution when the total net charge on a mineral particle vanishes. The PZC for kaolinite is 4.6 (Sparks, 2003), proto-imogolite allophane has a PZC of 6 to 7 (Gustafsson, 2001), and the PZC for the iron hydroxide, goethite, is $6.1 \pm 0.6$ (Sposito, 1984). Illite and chlorite, two other common layered aliminosilicate minerals found in soil, have a moderate to substantial percentage of ion exchange sites that are pH dependent and therefore probably have PZC values similar to that of kaolinite. Consequently, $NO_3^-$ mobility can potentially be reduced, through anion adsorption, in soils that have lower pH values and substantial amounts of kaolinite, illite, chlorite, allophane, and/or iron/aluminum oxides/hydroxides. For this $NO_3^-$ adsorption scenario to take place, there needs to be enough minerals with pH variable charge present to either completely dominate the clay-size fraction or at least coat a large percentage of soil surfaces. Anion adsorption of $NO_3^-$ has been documented for kaolinite-rich ultisols in the southeast United States (Eick et al., 1999; Toner et al., 1989), andisols containing large amounts of allophane (Katou et al., 1996; Ryan et al., 2001), and oxisols with iron/aluminum oxide/hydroxides from the tropics (Wong et al., 1990).

Electrostatic repulsion, or anion exclusion, occurs with $NO_3^-$ when ion exchange sites on soil mineral or organic matter surfaces are negatively charged. If anion exclusion processes dominate, $NO_3^-$ is repelled and does not come into contact with soil mineral and organic matter surfaces, and as a result, moves freely through the soil profile. Although pH dependent, the net charge on soil organic matter is always negative (Bohn et al., 1985). Dissociation of $H^+$ from carboxyl and phenol functional groups increases from low to high pH, causing a corresponding increase in the net negative charge of soil organic matter. Nearly all ion exchange sites on the layered aluminosilicate minerals, smectite and vermiculite, are considered permanent (not pH dependent) and negatively charged (Bohn et al., 1985). The PZC value for smectite (montmorillonite) is 2.5 (Sparks, 2003), and vermiculite probably has a PZC value that is similar. Therefore, not taking into account chemical and biological transformations, $NO_3^-$ is expected to move freely in soil environments with moderately low to high pH and significant amounts of organic matter, smectite, and/or vermiculite.

For most soils of the northern temperate zone, particle surfaces will have a negative charge resulting in anion exclusion as the dominant electrostatic interaction affecting $NO_3^-$ mobility. The range of cation exchange capacities (CEC) for kaolinite, illite, chlorite, vermiculite, and smectite are 1 to 15, 10 to 40, 20 to 40, 100 to 150, and 70 to 120 meq/100 g, respectively (Bohn et al., 1985; McBride, 1994). These CEC values show that for a given amount of material, the number of negatively charged ion exchange sites on vermiculite and smectite far outnumber the exchange sites for kaolinite, illite, and chlorite, implying that anion exclusion will be enhanced with increasing quantities of vermiculite and smectite. Quartz and other sand or silt-sized soil minerals have very low CEC values and will have minimal electrostatic interaction with $NO_3^-$.

Steady-state saturated and unsaturated soil column leaching experiments have been used to assess the anion exclusion effect by measuring the percentage of pore water unavailable for chloride ($Cl^-$) transport (Appelt et al., 1975; James and Rubin, 1986; Thomas and Swaboda, 1970). These studies indicate that the percentage of pore water excluded decreases with increased

$Cl^-$ concentration (Thomas and Swaboda, 1970) and becomes greater with larger soil CEC (Appelt et al., 1975). James and Rubin (1986) demonstrated that the percentage of pore water excluded increased as the overall water content was reduced, which resulted from the actual exclusion volume remaining constant. Furthermore, steady-state saturated column testing by Skulka and Cepuder (2000) showed the anion exclusion volume for $Cl^-$ to decrease as pore water velocity increased. Smith and Davis (1974) conducted steady-state unsaturated column tests on eight soils and found the percentage of excluded water ranged from 5% to 39% and was independent of whether the anion was bromide ($Br^-$) or $NO_3^-$. Melamed et al. (1994) demonstrated enhanced anion exclusion of $Br^-$ with reduction in PZC of an oxisol.

Bond and Phillips (1990) and Bond et al. (1982) quantified the anion exclusion effect on $Cl^-$ transport using constant-flux transient unsaturated horizontal column experiments carried out on a clayey soil having a moderate initial volumetric water content of 0.16 to 0.18. Phillips et al. (1988) conducted two transient unsaturated vertical column tests in dry soil, which showed that anion exclusion processes produced peak $Cl^-$ concentrations coinciding with the wetting front. Research at a larger scale with 6-m-long vertical soil columns and at field test plots confirm anion exclusion to impact the mobility of $Cl^-$, $Br^-$, and even sulfate (Gvirtzman et al., 1986; Hills et al., 1991; Porro and Wierenga, 1993; Porro et al., 1993).

Figure 1 depicts a pore-scale conceptualization of anion adsorption and anion exclusion processes under unsaturated flow conditions. The pore water velocity has a parabolic distribution based on the Hagen-Poiseuille law for laminar flow. From the side toward the center of the pore, the water velocity increases from zero at the soil/water interface and reaches a maximum value at the air/water interface. Based on electrostatic double layer theory (Hillel, 1980), anion adsorption processes will result in $NO_3^-$ becoming attached at or concentrated near the soil/water interface, whereas anion exclusion processes will involve $NO_3^-$ being repelled from the soil/water interface. Consequently, when anion adsorption processes dominate, $NO_3^-$ travels with the slower pore water, and when anion exclusion processes dominate, $NO_3^-$ moves with the faster pore water.

Overall, most research on anion mobility in soils has focused on the tracers $Cl^-$ and $Br^-$. With regard to $NO_3^-$, it appears there has been more investigation of $NO_3^-$ anion adsorption within very specific soil environments and much less directly devoted to understanding $NO_3^-$ anion exclusion. Because of the limited amount of soil $NO_3^-$ transport research focused on quantifying electrostatic interactions, along with growing concerns over environmental problems such as aquifer contamination in agricultural areas and the Gulf of Mexico hypoxic zone, there is a strong need for understanding of $NO_3^-$ mobility under unsaturated flow conditions in a variety of soil environments. Furthermore, computer models used to simulate N movement and transformations (Davidson et al., 1978; Hanson et al., 1999; Ma et al., 1999; Selim and Iskandar, 1981) in the soil profile could potentially be improved by incorporating $NO_3^-$ adsorption and exclusion processes, once there is a better understanding of these processes' impact in unsaturated soils. To address this research need, transient unsaturated horizontal column experiments were conducted to assess anion transport processes affecting $NO_3^-$ mobility in soil. The four soils chosen for testing, two from Oklahoma and two from Ohio, had widely different physicochemical and mineralogical properties. The two Oklahoma soils are representative of the Great Plains region where $NO_3^-$ contamination of shallow ground water is a major concern. The two Ohio soils are representative of the Midwest where soil drainage practices contribute to the Gulf of

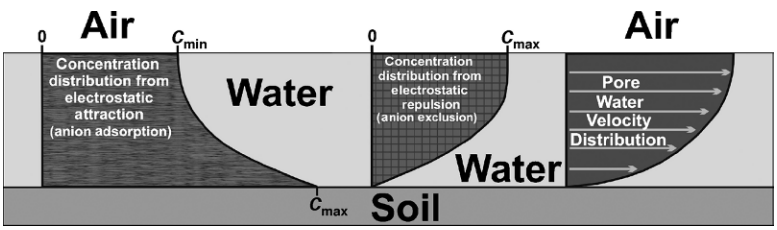


Fig. 1. Pore-scale conceptualization of anion adsorption and anion exclusion processes under unsaturated flow conditions.

TABLE 1
Soil physicochemical properties

| Soil | pH | OM[†] (%) | CEC[‡] (meq/100 g) | Sand (%) | Silt (%) | Clay (%) |
|---|---|---|---|---|---|---|
| Slaughterville | 7.19 | 0.14 | 5.16 | 75.8 | 15.2 | 9.0 |
| Teller | 6.10 | 2.03 | 15.92 | 35.3 | 41.1 | 23.6 |
| Hoytville | 5.84 | 3.17 | 24.40 | 13.0 | 42.8 | 44.2 |
| Paulding | 4.93 | 2.95 | 27.20 | 4.5 | 43.1 | 52.4 |

[†]OM = organic matter.
[‡]CEC = cation exchange capacity.

Mexico hypoxic zone problem. The governing hypothesis for this research project can be stated as follows: for the Ohio and Oklahoma soils tested, which are representative of many soils common to the northern temperate zone, anion exclusion will be a key process affecting $NO_3^-$ mobility under unsaturated flow conditions.

## MATERIALS AND METHODS

### *Soils*

The four soils used in this study were collected at a depth of 5 to 20 cm. Two soils were obtained near Perkins, OK, one from the Slaughterville series (course-loamy, mixed, superactive, thermic udic haplustolls) and one from the Teller series (fine-loamy, mixed, active, thermic udic argiustolls). Geographically, soils of the Teller and Slaughterville series are found in the Central Rolling Red Prairies within the Great Plains region of the United States. The two other soils tested came from Ohio. Soil from the Hoytville series (fine, illitic, mesic mollic epiaqualfs) was collected near Van Wert, OH, and soil from the Paulding series (very-fine, illitic, nonacid, mesic typic epiaquepts) was collected near Defiance, OH. Soils of the Hoytville and Paulding series were formed from sediments associated with glacial lakes of the Wisconsinan age.

Physicochemical properties of the four soils are provided in Table 1. Values for pH were determined from the soil solution of a saturated paste (US Department of Agriculture, 1954). The Walkley-Black method was used to measure organic matter content (Nelson and Sommers, 1982). Cation exchange capacity values were obtained by first saturating the exchange sites with sodium cations, followed by extraction of the sodium with a solution of ammonium acetate (Rhoades, 1982). Wray (1986) describes methods used to determine the soil particle size distribution. Based on classification of the particle size distribution, the Slaughterville soil is a sandy loam, the Teller soil is a loam, the Hoytville soil is a silty clay, and the Paulding soil is a silty clay. Table 1 shows that the Oklahoma soils had higher pH, lower organic matter (OM), smaller CEC, greater amounts of sand, and less clay than the soils from Ohio. In particular, the Slaughterville and Paulding soils, when compared with one another, exhibited the greatest differences in physicochemical properties.

The mineral composition for the clay-sized fraction of the four soils is given in Table 2. For this mineralogical analysis, the soil samples were first air dried and ground to pass a 2-mm sieve. Clay (<2 μm) fractions were obtained using standard sieve and gravity sedimentation techniques (Jackson, 1975; Rutledge et al., 1967). Subsamples were saturated with magnesium ($Mg^{2+}$) and potassium ($K^+$) and oriented aggregates were prepared using the filter transfer technique of Moore and Reynolds (1997). The $Mg^{2+}$- and $K^+$-saturated aggregates were then analyzed by x-ray diffraction as described by Ransom et al. (1988).

TABLE 2
Soil mineralogy (particle size <2 μm)[†]

| Soil | Illite (%) | Kaolinite (%) | Chlorite (%) | Vermiculite (%) | Smectite (%) | Quartz (%) | FeO[‡] (%) |
|---|---|---|---|---|---|---|---|
| Slaughterville | 30 | 15 | ~0 | 20 | 25 | <5 | ~5 |
| Teller | 35 | 25 | ~0 | 10 | 20 | 5 | ~5 |
| Hoytville | 40 | 10 | 10 | 15 | 15 | 5 | ~5 |
| Paulding | 45 | 15 | 20 | 10 | ~0 | 5 | ~5 |

[†]Mineralogy estimated from x-ray diffraction peaks. All samples had trace feldspar present.
[‡]FeO = iron oxide or iron hydroxide-goethite in Slaughterville, Teller, and Hoytville soils and lepidocrocite in Paulding soil.

For the clay-size fraction, Table 2 shows the highest smectite percentages in the Oklahoma soils, whereas and illite and chlorite percentages were highest in the Ohio soils. The Oklahoma soils, in fact, had no measurable chlorite. The Paulding soil differed significantly from the others by having no smectite, the greatest amount of chlorite (20% of clay-sized fraction), and, in regard to iron oxides/hydroxides, lepidocrocite instead of goethite.

*Laboratory Testing of Nitrate Transport*

Nitrate mobility under unsaturated flow conditions was assessed using transient unsaturated horizontal column experiments. Transient unsaturated horizontal flow in a soil column can be described by the relationship:

$$\frac{\partial\theta}{\partial t} = \frac{\partial}{\partial x}\left(D(\theta)\frac{\partial\theta}{\partial x}\right) \tag{1}$$

where $t$ is time ($T$) from test initiation, $x$ is distance ($L$) from the column inlet, $\theta$ is volumetric water content (dimensionless), and $D(\theta)$ is the soil water diffusivity ($L^2/T$), itself a function of $\theta$. Soil water diffusivity can in turn be expressed:

$$D(\theta) = K(\theta)\frac{\partial\psi}{\partial\theta} \tag{2}$$

where $\psi$ is pore water pressure potential ($L$), and $K(\theta)$ is unsaturated hydraulic conductivity ($L/T$), which is dependent on $\theta$. Bruce and Klute (1956) showed that by using the Boltzmann transform, $\lambda = x/\sqrt{t}$, having dimensions $L/T^{0.5}$, Eq. (1) can be reduced to an ordinary differential equation of the form:

$$-\frac{\lambda}{2}\frac{d\theta}{d\lambda} = \frac{d}{d\lambda}\left(D(\theta)\frac{d\theta}{d\lambda}\right) \tag{3}$$

Using the following boundary conditions,

$$\theta = \theta_i, \text{ for } \lambda \to \infty \ (x \to \infty \text{ or } t = 0), \text{ and} \tag{4}$$

$$\theta = \theta_0, \text{ for } \lambda = 0 \ (x = 0 \text{ and } t > 0) \tag{5}$$

the diffusivity versus water content relationship can be determined from transient unsaturated horizontal column experiments. The boundary condition given by Eq. (4) simply indicates that the volumetric water content beyond the wetting front is the same as the initial volumetric water content, $\theta_i$, of the soil column. The second boundary condition, Eq. (5), states that the volumetric water content at the inlet of the soil column, $\theta_0$, is kept constant throughout the test. Given these two hydraulic boundary conditions, Eq. (3) can be integrated with respect to $\lambda$ and soil water diffusivity calculated over a range of water content values using soil column moisture profile data. This soil water diffusivity relationship is expressed as

$$D(\theta_*) = -\frac{1}{2}\left(\frac{d\lambda}{d\theta}\right)_{\theta_*}\int_{\theta_i}^{\theta_*}\lambda d\theta \tag{6}$$

where $\theta_*$ is an arbitrary water content between $\theta_i$ and $\theta_0$, and the term $\left(>\frac{d\lambda}{d\theta}\right)_{\theta_*}$ represents the derivative of $\lambda$ with respect to $\theta$ at $\theta = \theta_*$ (Bruce and Klute, 1956).

A computer-controlled syringe pump apparatus described by Brown and Allred (1992) and shown in Figure 2 was used to inject a 200-mg/L $NO_3^-$-N solution (1.44 g $KNO_3$/L) into the inlet of dry soil columns. Using a computer-controlled syringe pump allowed the volumetric water content at the column inlet to be maintained at a constant value [Eq. (5)] throughout the time duration of the test. The boundary condition of Eq. (5) was accomplished by regulating the instantaneous injected flow at a rate inversely proportional to the square root of elapsed time. The specific equation for the instantaneous injected flow rate, $Q$ ($L^3$/T), is:

$$Q = \frac{1}{2}ASt^{-\frac{1}{2}} \tag{7}$$

where $A$ is the cross-sectional area of the soil column ($L^2$), $S$ is the sorptivity ($L/T^{0.5}$), and $t$ is again the time ($T$) since the experiment began. Sorptivity can be expressed in the following forms:

$$S = \int_{\theta_i}^{\theta_0}\lambda d\theta = \frac{V}{A}t_T^{-\frac{1}{2}} \tag{8}$$

where $V$ is the total volume ($L^3$) of the of the solution injected at the inlet of the soil column, and $t_T$ is the total test duration time (Brown and Allred, 1992). Substituting the last term in Eq. (8) into Eq. (7) yields:

$$Q = \frac{1}{2}(Vt_T^{-\frac{1}{2}})t^{-\frac{1}{2}} \tag{9}$$

showing that the proportionality constant between Q and $t^{-\frac{1}{2}}$ in the injection rate relationship is simply a function of the chosen injection volume and test duration that are both input into the computer controlling the syringe pump. Consequently, for consistency between experiments, the same $S$ of 0.0073 cm/sec$^{0.5}$ and $A$ of 9.35 cm$^2$ was used in each column experiment, thereby giving a consistent instantaneous injection rate of

$$Q = 0.034t^{-\frac{1}{2}}\ (cm^3/sec) \tag{10}$$

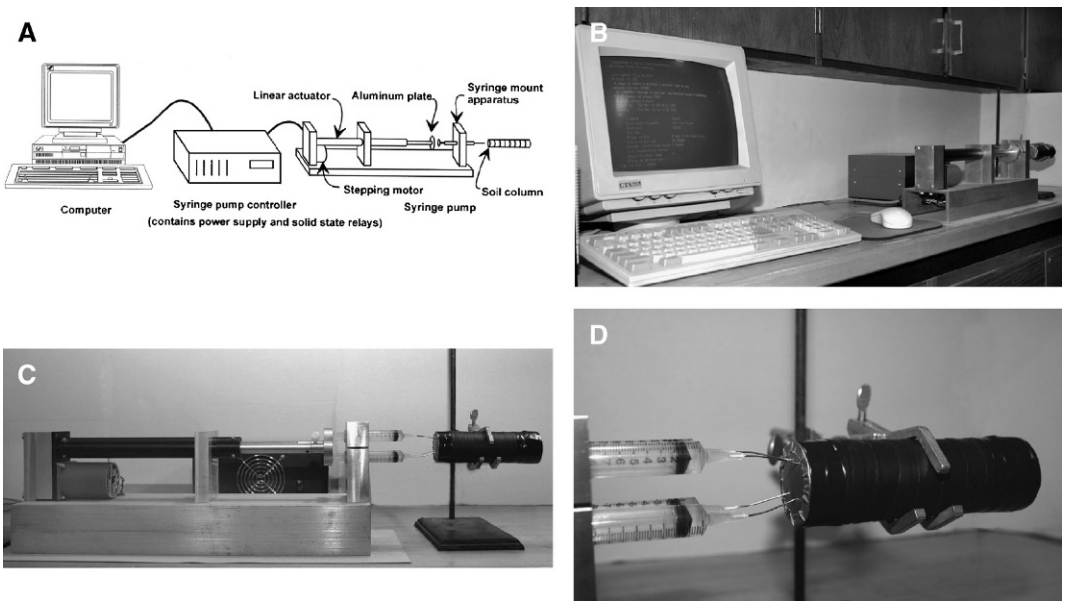


Fig. 2. (A) Schematic of computer-controlled syringe pump apparatus, (B) photo of computer-controlled syringe pump apparatus, (C) close-up photo of syringe pump and horizontal soil column with controller in background, and (D) close-up of syringes inserted into column inlet.

At this point, it is important to note that the actual value of the inlet volumetric water content maintained during a test depends not only on the programmed injection rate function but also soil hydraulic properties.

The column itself was comprised of individual acrylic rings (Fig. 2) and packed with one of the four soils previously described. The individual rings had an inside diameter of 3.45 cm and were 1 cm in length. Total column length ranged from 12 to 20 cm. Before being packed into the column, each of the four soils were washed with a 2 *M* calcium chloride solution to saturate cation exchange sites with calcium ions and to displace any adsorbed $NO_3^-$. This initial wash was followed by six additional washes with distilled water to remove excess salts and any $NO_3^-$ originally in the soil. After the complete washing cycle, each soil was placed in an oven and dried at 50 °C and then ground to pass a 2-mm sieve. The columns, after being packed with soil 1 cm at a time, were sealed at the ends with duct tape and along their length with self-fusing rubber splicing tape to prevent evaporative losses during testing.

Each test, as indicated previously, was programmed for a set time duration and 200 mg/L of $NO_3^-$-N solution (1.44 g $KNO_3$/L) injection volume. Two tests were conducted for each of the four soils to determine if results could be replicated. The two tests for a particular soil had different time durations and solution injection volumes, but as already discussed, the same sorptivity, injection rate function, and hence,

TABLE 3
Test parameters

| Soil-test number | Column length (cm) | Time duration (h) | Solution injection volume (mL) | Packed dry bulk density (g/mL) | $\theta_i$ |
|---|---|---|---|---|---|
| Slaughterville-1 | 12 | 12.0 | 14.14 | 1.695 | 0.0027 |
| Slaughterville-2 | 20 | 24.0 | 20.00 | 1.688 | 0.0019 |
| Teller-1 | 12 | 12.0 | 14.14 | 1.586 | 0.0029 |
| Teller-2 | 20 | 24.0 | 20.00 | 1.585 | 0.0022 |
| Hoytville-1 | 17 | 24.0 | 20.00 | 1.509 | 0.0364 |
| Hoytville-2 | 15 | 48.0 | 28.28 | 1.512 | 0.0366 |
| Paulding-1 | 15 | 24.0 | 20.00 | 1.496 | 0.0487 |
| Paulding-2 | 15 | 40.5 | 26.30 | 1.494 | 0.0463 |

inlet water content, $\theta_0$. Table 3 provides information on column length, time duration, injection volume, dry bulk density, and initial water content, $\theta_i$, for all eight tests carried out in this investigation. Table 3 indicates that both tests for a given soil had essentially the same column packing density and $\theta_i$ [boundary condition of Eq. (4)]. The Hoytville and Paulding soils, although still relatively dry, had $\theta_i$ values substantially greater than the Slaughterville and Teller soils, which were extremely dry. The uniform dry bulk packing densities of the Hoytville and Paulding soil columns were marginally less than the dry bulk packing densities of the Slaughterville and Teller soil columns.

Upon test completion, the soil from within each ring was divided into two parts, one for analysis of volumetric water content and the other for determination of $NO_3^-$-N concentration in the soil solution. Volumetric water content values were calculated based on the weight of the column soil samples before and after oven drying for 24 h at 105 °C. The mean of the injected water accounted for by oven drying, for all eight tests, was 97.5%, with a standard deviation of 0.9%. Soil samples for determining soil solution $NO_3^-$-N concentration were placed in 50-mL centrifuge tubes and 45 mL of 1 *M* KCl solution then added to disperse soil particles and desorb $NO_3^-$. These centrifuge tubes containing soil and solution were next placed on a shaker at 300 rpm for 1 h to obtain thorough mixing. After being shaken, each mixture of soil and solution was centrifuged at 800*g* (2500 rpm) for 1 h. After the centrifuge step, soil and solution were refrigerated. The final step involved filtering, and then analyzing the centrifuged solutions for $NO_3^-$-N with a Lachat Instruments QuikChem 8000 Flow Injection Analysis System (Milwaukee, WI) using a modified version of the cadmium reduction column method (US Environmental Protection Agency, 1979). For all eight experiments, an average value of 102.5% of the injected $NO_3^-$-N was accounted for by laboratory analysis, with a standard deviation of 2.2%.

### *Data Analysis*

Volumetric water content and soil solution $NO_3^-$-N concentration values from each experiment were plotted with respect to the Boltzmann transform (distance from the column inlet divided by the square root of the test duration time). Calculation of soil water diffusivity values [Eq. (6)] and, most importantly, assessment of $NO_3^-$ adsorption or exclusion processes was based on data from the column profiles for volumetric water content and soil solution $NO_3^-$-N concentration. Hypothetical volumetric water content and soil solution $NO_3^-$-N profiles plotted versus the Boltzmann transform are shown in Figure 3. These hypothetical transient unsaturated horizontal column profiles are representative of soil materials that are initially dry and have no $NO_3^-$ present. From research previously discussed, there are

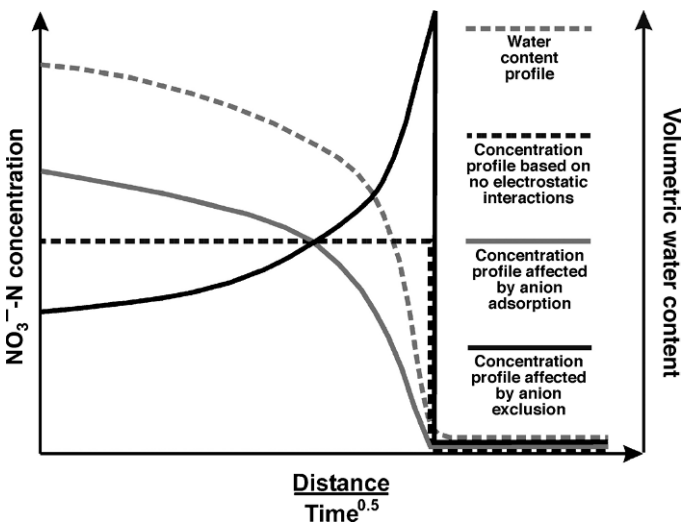


Fig. 3. Ideal transient unsaturated horizontal column water content and soil solution $NO_3^-$-N concentration profiles for an initially dry soil.

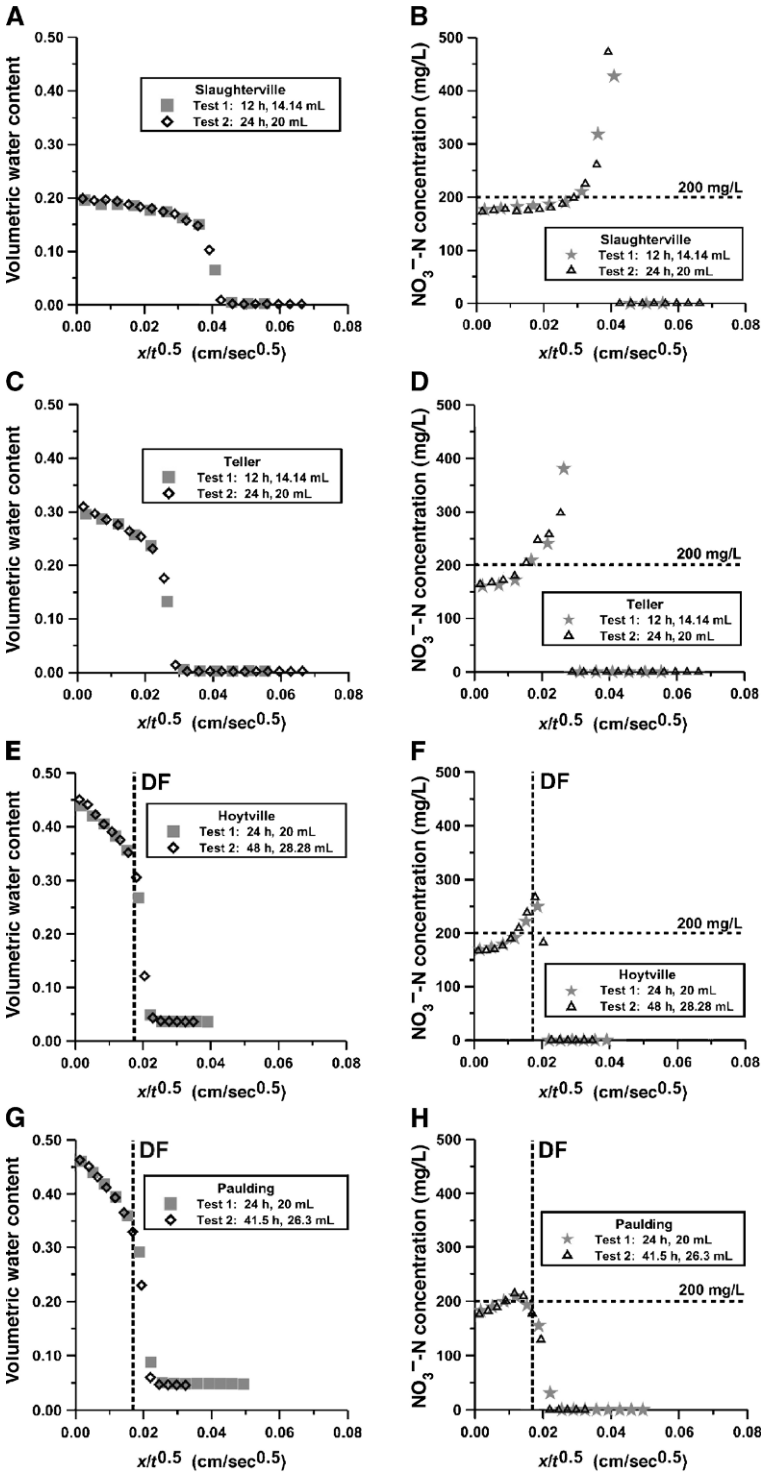


Fig. 4. Experimental data profiles: (A) Slaughterville water content, (B) Slaughterville $NO_3^-$-N concentration, (C) Teller water content, (D) Teller $NO_3^-$-N concentration, (E) Hoytville water content, (F) Hoytville $NO_3^-$-N concentration, (G) Paulding water content, and (H) Paulding $NO_3^-$-N concentration. Dashed vertical lines labeled DF represent the position of the theoretical displacement front between injected water and displaced initial water.

three hypothetical $NO_3^-$-N concentration profiles, one based on no electrostatic interactions, one due to anion adsorption, and one the result of anion exclusion (Fig. 3). Given no electrostatic interactions between $NO_3^-$ and soil surfaces, the $NO_3^-$-N soil solution concentration profile will have a constant value from the column inlet to the wetting front, and this concentration will equal that of the original injected solution.

The dominance of anion adsorption processes results in a $NO_3^-$-N concentration profile having its greatest value at the column inlet and with distance from the inlet, tailing off to zero at the wetting front (Fig. 3). Alternatively, if the positively charged exchange sites near the inlet become saturated with $NO_3^-$, then the $NO_3^-$-N concentration profile will maintain a constant value for some distance from the column inlet before dropping to zero at the wetting front. In either of the anion adsorption scenarios, the highest $NO_3^-$-N values reported with respect to the soil solution are adjacent to the inlet and greater in magnitude than the $NO_3^-$-N concentration of the original injected solution. When anion exclusion is the dominant electrostatic interaction, $NO_3^-$ is repelled from soil surfaces and moves with the fastest pore water, thereby causing an $NO_3^-$-N concentration peak to occur at the wetting front and the lowest $NO_3^-$-N values to be located near the inlet. The magnitude of the wetting front $NO_3^-$-N concentration peak produced by anion exclusion will be significantly greater than the $NO_3^-$-N concentration of the original injected solution, whereas at the column inlet, soil solution $NO_3^-$-N values will be less than the $NO_3^-$-N concentration of the original injected solution.

A simple method for numerically determining whether anion adsorption or anion exclusion processes dominate $NO_3^-$ transport in unsaturated soil columns involves comparing $X_C$ (Boltzmann transform value at the centroid of an column test $NO_3^-$-N concentration profile) to $X_{C\text{-}NEI}$ (Boltzmann transform value at the centroid for a theoretical $NO_3^-$-N concentration profile based on no electrostatic interactions). The calculation for $X_{C\text{-}NEI}$ assumes the same wetting front (or displacement front) penetration as was obtained with the actual experiment. If $X_C < X_{C\text{-}NEI}$, then anion adsorption is indicated, and if $X_C > X_{C\text{-}NEI}$, then anion exclusion is implied.

The magnitude of the anion exclusion effect in a transient unsaturated horizontal column experiment can be quantified several ways. Anion exclusion, as stated before, involves $NO_3^-$ being repelled from soil surfaces and moving with the faster pore water velocities, in turn causing the $NO_3^-$-N concentration near the column inlet, $C_0$, to be less than the $NO_3^-$-N concentration of the original injected solution, $C_{orig}$. Therefore, one measure of the magnitude of the anion exclusion effect is the ratio, $C_0/C_{orig}$. The ratio, $C_0/C_{orig}$, can then be used to calculate the effective excluded pore water volume at the inlet, $\theta_{ex}$, that is unavailable to $NO_3^-$. The value of $\theta_{ex}$ is calculated by (Fetter, 1993):

$$\theta_{ex} = \theta_0 \left(1 - \left(\frac{C_0}{C_{orig}}\right)\right) \tag{11}$$

where $\theta_0$, as previously defined, is the volumetric water content at the column inlet. The proportion of inlet water content that is excluded becomes simply $\theta_{ex}/\theta_0$. Because anion exclusion results in $C_0 < C_{orig}$, then given sufficiently dry initial soil conditions, mass balance considerations alone indicate that there will be some soil solution $NO_3^-$-N concentrations greater than $C_{orig}$. Therefore, the ratio of the maximum soil solution $NO_3^-$-N concentration to $C_{orig}$, or $C_{max}/C_{orig}$, is another valid measure of the magnitude of the anion exclusion effect. (Note: If $X_C < X_{C\text{-}NEI}$, then $C_{max}/C_{orig}$ becomes a valid measure of the magnitude of anion adsorption.) As defined by these quantities, the larger the apparent $NO_3^-$ anion exclusion effect, the smaller the value of $C_0/C_{orig}$, the greater the value of $\theta_{ex}$, the larger the value of $\theta_{ex}/\theta_0$, and the greater the value of $C_{max}/C_{orig}$.

## RESULTS AND DISCUSSION

Profiles of the transient unsaturated horizontal column experimental data are provided in Figure 4. Again, water content and $NO_3^-$-N concentration values are plotted with respect to the Boltzmann transform (distance from the column inlet divided by the square root of the test duration time). For each soil, different symbols are used to distinguish data of the first test from data of the second test. The two column experiments for each soil, as previously discussed, had the same hydraulic boundary conditions but different time durations and $NO_3^-$-N solution injection volumes. It is quite apparent from Figure 4, given a particular soil, that similarity exists between the two water

content profiles, and similarity exists between the two $NO_3^-$-N concentration profiles. This observed similarity has some very important implications. First, the similarity exhibited is clear evidence that the results are very repeatable. Second, with regard to soil volumetric water content, similar profiles indicate that water/soil interactions quickly achieved equilibrium, a constant inlet water content boundary condition [Eq. (5)] was maintained, and as a consequence, Eq. (6) is applicable for calculating soil water diffusivity. Finally, similarity of the $NO_3^-$-N concentration profiles implies that, for a particular soil, chemical interactions involving $NO_3^-$ were reversible with equilibrium conditions rapidly reached.

Nitrate-nitrogen concentration profile similarity additionally indicates that the $NO_3^-$-N inlet concentration remains constant throughout the test. Consequently, the $NO_3^-$-N concentration ($C$) boundary conditions for the tests conducted in this study can be expressed as follows:

$$C \cong 0, \text{ for } \lambda \to \infty (x \to \infty \text{ or } t = 0), \text{ and} \quad (12)$$

$$C = C_0, \text{ for } \lambda = 0 \ (x = 0 \text{ and } t > 0) \quad (13)$$

The boundary condition given by Eq. (12) indicates that the initial $NO_3^-$-N concentration in soil column is essentially zero. The second boundary condition, Eq. (13), states that the $NO_3^-$-N inlet concentration is kept constant throughout the test.

The Hoytville and Paulding soils, although relatively dry, had values of initial volumetric water content, $\theta_i$, which were greater than the extremely dry Slaughterville and Teller soils (Table 3). Consequently, there was a small but significant amount of initial water displaced during experiments conducted with the Hoytville and Paulding soils. The position of the theoretical displacement front (Smiles and Philip, 1978) between the injected water and the displaced initial water is indicated by the vertical dashed lines labeled DF in Figures 4E–H. For the Hoytville soil, this theoretical displacement front, which discounting mixing, occurs at a Boltzmann transform value of 0.0174 cm/sec$^{0.5}$, and for the Paulding, the displacement front is found at a Boltzmann transform value of 0.0169 cm/sec$^{0.5}$.

Data from both column tests for each soil were used to construct a composite volumetric water content profile and a composite soil solution $NO_3^-$-N concentration profile for each soil. These composite profiles for all four soils are displayed in Figure 5. The composite soil volumetric water content profiles (Fig. 5A) show that the wetting front penetrated furthest in the Slaughterville soil, followed next by the Teller soil, with the Hoytville and Paulding soils being equal and having the least wetting front penetration. This wetting penetration trend is quantified by calculating, $X_W$, the Boltzmann transform value at the water content profile centroid. As is the case for the wetting front positions in Figure 5A, Table 4 shows that $X_W$ is greatest by far for the Slaughterville soil (0.0192 cm/sec$^{0.5}$), and the Teller soil is next in magnitude (0.0127 cm/sec$^{0.5}$), with the Hoytville and Paulding soils having the smallest $X_W$ values of 0.0097 and 0.0100 cm/sec$^{0.5}$, respectively. The inlet water content values, $\theta_0$, were highest for the Paulding and Hoytville soils, approximately 0.47 and 0.45, respectively (Fig. 5A and Table 4). The Teller soil had a $\theta_0$ of around 0.3, and the Slaughterville soil had the lowest $\theta_0$ of about 0.2 (Fig. 5A and Table 4).

The composite volumetric water content profiles in Figure 5A were used with Eq. (6) to determine the diffusivity versus volumetric water content relationships for each soil. These soil water diffusivity versus volumetric water content relationships are depicted in Figure 6. The range of soil water diffusivity values are $1 \times 10^{-5}$ to $1 \times 10^{-2}$ cm$^2$/sec for the Slaughterville soil, $8 \times 10^{-6}$ to $2 \times 10^{-3}$ cm$^2$/sec for the Teller soil, and $6 \times 10^{-6}$ to $8 \times 10^{-4}$ cm$^2$/sec for both Hoytville and Paulding soils. Figure 6 indicates, given a particular range of volumetric water content, that diffusivities are highest with the Slaughterville soil, with the Teller soil next, and with the Hoytville and Paulding soils having similar diffusivities that are substantially lower than the other two soils. Wetting front penetration, inlet water content, and diffusivity values all indicate that water is capable of moving faster through the Oklahoma soils (Slaughterville and Teller) than the Ohio soils (Hoytville and Paulding), a result most likely due to the Oklahoma soils having a much lower percentage of clay-sized particles than the Ohio soils (Table 1). Water drains very quickly through the Slaughterville soil, and fertilizer applied to this soil will have the potential to cause $NO_3^-$ contamination in underlying aquifers, especially if anion exclusion strongly affects $NO_3^-$ transport.

The configuration of the Slaughterville, Teller, and Hoytville soil solution $NO_3^-$-N concentration profiles (Fig. 5B) are very similar

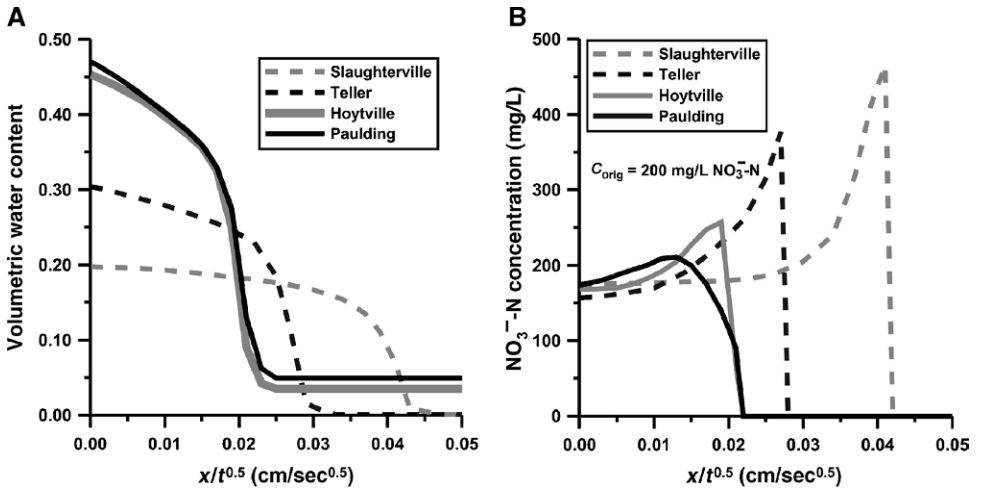


Fig. 5. Composite experimental result profiles plotted versus the Boltzmann transform: (A) volumetric water content and (B) soil solution $NO_3^-$-N concentration.

to that of the hypothetical anion exclusion affected $NO_3^-$-N concentration profile displayed in Figure 3. Specifically, the lowest $NO_3^-$-N concentrations for all three soils were adjacent to the column inlet, and the highest $NO_3^-$-N concentrations for the Slaughterville and Teller soils were found in a peaks positioned at the wetting fronts (Fig. 5A), whereas the highest $NO_3^-$-N concentrations for the Hoytville soil were found in a peak positioned between the theoretical displacement front and the wetting front (see Figs. 4 and 5B). Additionally, $X_C > X_{XC\text{-}NEI}$ for the Slaughterville, Teller, and Hoytville soils (Table 4). Consequently, there is little doubt that anion exclusion is the dominant electrostatic interaction impacting $NO_3^-$ mobility in these soils. This result is not surprising, because as shown in Tables 1 and 2 for the Slaughterville, Teller, and Hoytville soils, pH conditions were fairly neutral (~6-7), and the clay-sized fractions contained significant quantities of smectite and vermiculite (30%–45%).

Regarding these three soils and the quantities used to gauge the magnitude of the anion exclusion effect (Table 4), the Slaughterville soil has the greatest value of $C_{max}/C_{orig}$ (2.33), the Teller soil has the smallest value of $C_0/C_{orig}$ (0.79) and the largest value of $\theta_{ex}/\theta_0$ (0.214), and the Hoytville soil has the greatest value of

TABLE 4

Water content and $NO_3^-$ concentration characteristics of the soil column tests[†]

| Soil | $\theta_0$[‡] | $\theta_{ex}$[§] | $\theta_{ex}/\theta_0$ | $C_0/C_{orig}$[¶] | $C_{max}//C_{orig}$[‖] | $X_W$[#] ($cm/sec^{0.5}$) | $X_{C\text{-}NEI}$[††] ($cm/sec^{0.5}$) | $X_C$[‡‡] ($cm/sec^{0.5}$) |
|---|---|---|---|---|---|---|---|---|
| Slaughterville | 0.198 | 0.026 | 0.131 | 0.87 | 2.33 | 0.0192 | 0.0210 | 0.0242 |
| Teller | 0.304 | 0.065 | 0.214 | 0.79 | 1.89 | 0.0127 | 0.0140 | 0.0162 |
| Hoytville | 0.453 | 0.072 | 0.159 | 0.84 | 1.30 | 0.0097 | 0.0087 | 0.0112 |
| Paulding | 0.470 | 0.061 | 0.130 | 0.87 | 1.06 | 0.0100 | 0.0085 | 0.0104 |

[†]Values determined from composite profiles for water content and $NO_3^-$-N concentration.

[‡]$\theta_0$ = volumetric water content at inlet of soil columns during testing.

[§]$\theta_{ex}$ = excluded volumetric water content at inlet of soil columns during testing.

[¶]$C_0/C_{orig}$ = ratio of soil solution $NO_3^-$-N concentration at inlet to original injected $NO_3^-$-N solution concentration ($C_{orig}$ = 200 mg/L $NO_3^-$-N ).

[‖]$C_{max}/C_{orig}$ = ratio of maximum soil solution $NO_3^-$-N concentration to original injected $NO_3^-$N solution concentration.

[#]$X_M$ = Boltzmann transform value at centroid of volumetric water content profile.

[††]$X_{C\text{-}NEI}$ = Boltzmann transform value at centroid of theoretical $NO_3^-$-N concentration profile assuming no electrostatic interactions (based on the wetting front position for the Slaughterville and Teller soils and based on the theoretical displacement front position for the Hoytville and Paulding soils).

[‡‡]$X_C$ = Boltzmann transform value at centroid of column test $NO_3^-$-N concentration profile.

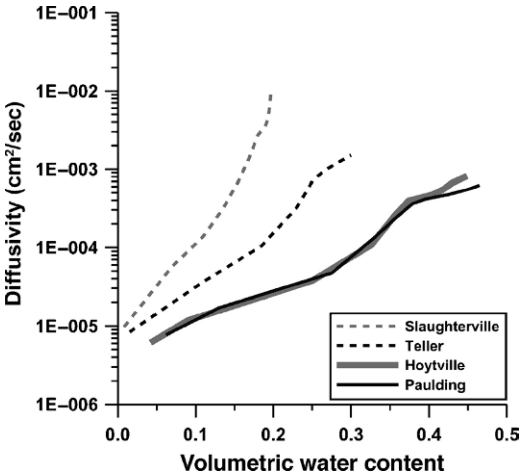


Fig. 6. Soil water diffusivity versus volumetric water content relationships.

$\theta_{ex}$ (0.072). Based solely on these quantities, it is difficult to determine which of the three soils had the largest anion exclusion impact on $NO_3^-$ mobility. Consequently, using Eq. (11) as a starting point, a somewhat different testing approach may be required to better compare $NO_3^-$ anion exclusion effects between various soils. This different testing approach, instead of using a constant injection rate function [such as Eq. (10)] for all soils as was done in this study, would alternatively adjust the injection rate function used for each soil so that the inlet moisture content, $\theta_0$, is maintained at a constant value for all experiments, regardless of the particular soil being tested. With adoption of this approach, comparisons of inlet $NO_3^-$-N concentrations is all that is needed to evaluate differences in $NO_3^-$ anion exclusion effects for various soils.

It is interesting to note that the peak $NO_3^-$-N concentrations that occurred at the wetting front for both the Slaughterville and the Teller soils were approximately twice the concentration of the 200-mg/L $NO_3^-$-N solution injected at the column inlet. These results demonstrate that in dry soils, anion exclusion not only makes $NO_3^-$ more mobile, but can potentially produce high concentration $NO_3^-$ "pulses" that move through the soil profile. $NO_3^-$-N concentration profile results for the Slaughterville soil, which was almost completely devoid of organic matter (0.14%), indicates that the clay minerals alone can produce a substantial anion exclusion effect. The Hoytville soil was marginally wetter than the very dry Slaughterville or Teller soils (Table 3), and as a consequence of both anion exclusion and dispersion (mechanical mixing and predominantly molecular diffusion) processes, the peak soil solution $NO_3^-$-N concentration for the Hoytville soil, after very close inspection of Figure 4E and F, was found to occur between the theoretical displacement front and the actual wetting front. Under these somewhat wetter conditions, dispersion undoubtedly reduced the peak soil solution $NO_3^-$-N concentration in the slightly wet Hoytville soil compared with the peak soil solution $NO_3^-$-N concentration, which would have been achieved if the Hoytville soil was completely dry.

The Paulding soil had a soil solution $NO_3^-$-N concentration profile that was different than any of the three hypothetical $NO_3^-$-N concentration profiles presented in Figure 3. Table 4 shows that $X_C > X_{NEI}$, clear evidence that anion exclusion is the most important electrostatic interaction affecting $NO_3^-$ mobility in the Paulding soil. Furthermore, as depicted in Figures 4H and 5B, $NO_3^-$-N concentration values adjacent to the inlet of the Paulding soil columns were lower than the 200-mg/L $NO_3^-$-N concentration of the original injected solution. Consequently, the Paulding soil $NO_3^-$-N concentration condition at the inlet conformed to the inlet $NO_3^-$-N concentration condition expected for anion exclusion, specifically $C_0/C_{orig} < 0$. The $C_0/C_{orig}$ for the Paulding soil equaled 0.87 (Table 4). It is the position of the peak $NO_3^-$-N concentration, however, that is somewhat puzzling. The Paulding had an initial water content equal to approximately 0.048 (Table 3), and based on both anion exclusion and this modest initial moisture content, the peak $NO_3^-$-N concentration was expected, like the Hoytville soil, to be found somewhere between the theoretical displacement front and the wetting front. In actuality, the peak $NO_3^-$-N concentration for the Paulding soil was found at a Boltzmann transform value of 0.012 cm/sec$^{0.5}$, which is well behind both the theoretical displacement front located at a Boltzmann transform value of 0.0169 cm/sec$^{0.5}$ and the wetting front located at a Boltzmann transform value of 0.021 cm/sec$^{0.5}$ (Figs. 4G and H and 5B).

It is unclear as to exactly why the Paulding soil solution $NO_3^-$-N concentration profile exhibited this pattern. Dispersion, without question, played a major role. An additional factor might include anion adsorption and anion exclusion processes operating simultaneously, with

the anion exclusion process being moderately stronger. This possibility, with regard to the Paulding soil, of anion adsorption and anion exclusion processes competing simultaneously, is plausible based on soil conditions presented in Tables 1 and 2. The Paulding soil had a fairly low pH (4.93), providing the prospect that the lepidocrocite and maybe even the kaolinite minerals present (20% of the total clay-sized fraction) could have been positively charged. The Paulding soil had no smectite, but the vermiculite that was present (10% of the total clay-sized fraction), even at a low pH value of 4.93, would still most likely have had a strong negative charge. Consequently, the Paulding soil may have had significant amounts of both positively and negatively charged soil particles affecting $NO_3^-$ mobility.

## SUMMARY AND CONCLUSIONS

Growing environmental concerns, such as $NO_3^-$ contamination of aquifers and the Gulf of Mexico hypoxic zone, suggest the need for a better understanding of processes affecting $NO_3^-$ mobility in soil. Nitrate mobility within the soil environment is governed to a significant extent by electrostatic interactions between negatively charged $NO_3^-$ ions and charged soil particle surfaces (either mineral or organic). Anion adsorption occurs when $NO_3^-$ ions become attracted to positively charged exchange sites on a soil surface. When anion exclusion processes dominate, $NO_3^-$ ions are repelled from soil particle surfaces and move with the fastest pore water velocity. Transient unsaturated horizontal column experiments were conducted to assess electrostatic processes affecting $NO_3^-$ transport in soil under initially dry conditions. Duplicate tests were conducted on four soils having different physicochemical and mineralogical properties. The four soils investigated were a Slaughterville sandy loam and a Teller loam from Oklahoma along with a Hoytville silty clay and a Paulding silty clay from Ohio. The two Oklahoma soils are representative of the Great Plains region where $NO_3^-$ contamination of shallow ground water is a major concern, and the two Ohio soils are typical of those found in the Midwest where agricultural practices contribute to the Gulf of Mexico hypoxic zone problem. In each test, a 200-mg/L $NO_3^-$-N solution was applied at the inlet of the relatively dry soil columns using the same injection rate function.

Comparison of corresponding volumetric water content and soil solution $NO_3^-$-N concentration profiles from the column tests clearly indicate anion exclusion to be the most important electrostatic process impacting $NO_3^-$ mobility under unsaturated flow conditions. Evidence of anion exclusion for all four soils includes soil solution $NO_3^-$-N concentrations near the column inlet that were 13% to 21% less than the 200 mg/L $NO_3^-$-N solution concentration originally injected into the column. Further strong anion exclusion evidence includes peak soil solution $NO_3^-$-N concentrations that were greater than 200 mg/L (sometimes by a factor of 2) found at or very near the wetting front for the Slaughterville, Teller, and Hoytville soils. Consequently, anion exclusion processes can produce high concentration $NO_3^-$ "pulses" that move through dry soils. The Paulding soil, possibly due to a combination of dispersion processes, low pH, and the mixture of clay minerals present, behaved somewhat differently than the other soils by having a peak soil solution $NO_3^-$-N concentration above 200 mg/L located approximately halfway between the column inlet and wetting front. Overall research results indicate that anion exclusion is a key process affecting $NO_3^-$ mobility in soils common to the northern temperate zone.

## ACKNOWLEDGMENTS

The authors thank Dedra Woner for conducting the soil nitrate analysis and Sandy Jones for the soil mineralogy laboratory work.

## REFERENCES

Appelt, H., K. Holtzclaw, and P. F. Pratt. 1975. Effect of anion exclusion on the movement of chloride through soils. Soil Sci. Soc. Am. Proc. 39(2):264–267.

Bohn, H. L., B. L. McNeal, and G. A. O'Connor. 1985. Soil Chemistry, 2nd Ed. John Wiley & Sons, New York, NY.

Bond, W. J., B. N. Gardiner, and D. E. Smiles. 1982. Constant-flux absorption of a tritiated calcium chloride solution by a clay soil with anion exclusion. Soil Sci. Soc. Am. J. 46(6):1133–1137.

Bond, W. J., and I. R. Phillips. 1990. Ion transport during unsteady water flow in an unsaturated clay soil. Soil Sci. Soc. Am. J. 54(3):636–645.

Brown, G. O., and B. Allred. 1992. The performance of syringe pumps in unsaturated horizontal column experiments. Soil Sci. 154:243–249.

Bruce, R. R., and A. Klute. 1956. The measurement of soil moisture diffusivity. Soil Sci. Soc. Am. Proc. 20:458–462.

Davidson, J. M., D. A. Graetz, P. S. C. Rao, and H. M. Selim. 1978. Simulation of nitrogen movement, transformation, and uptake in plant root zone. Technical Report EPA-600/3-78-029. US Environmental Protection Agency, Athens, GA.

Eick, M. J., W. D. Brady, and C. K. Lynch. 1999. Charge properties and nitrate adsorption of some acid Southeastern soils. J. Environ. Qual. 28(1): 138–144.

Fetter, C. W. 1993. Contaminant Hydrogeology. Macmillan, New York, NY.

Foth, H. D. 1984. Fundamentals of Soil Science, 7th Ed. John Wiley & Sons, New York, NY.

Freeze, R. A., and J. A. Cherry. 1979. Groundwater. Prentice-Hall, Englewood Cliffs, NJ.

Goolsby, D. A., and W. A. Battaglin. 2000. Nitrogen in the Mississippi Basin-estimating sources and predicting flux to the Gulf of Mexico. US Geological Survey Fact Sheet 135-00, Reston, VA.

Gustafsson, J. P. 2001. Modelling competitive anion adsorption on oxide minerals and an allophane-containing soil. Eur. J. Soil Sci. 52(4)639–653.

Gvirtzman, H., D. Ronen, and M. Magaritz. 1986. Anion exclusion during transport through the unsaturated zone. J. Hydrol. 87(3/4):267–283.

Hanson, J. D., K. W. Rojas, and M. J. Shaffer. 1999. Calibrating the root zone water quality model. Agron. J. 91:171–177.

Hillel, D. 1980. Fundamentals of Soil Physics. Academic Press, San Diego, CA.

Hills, R. G., P. J. Wierenga, D. B. Hudson, and M. R. Kirkland. 1991. The second Las Cruces experiment: Experimental results and two-dimensional flow prediction. Water Res. Res. 27(10):2707–2718.

Jackson, M. L. 1975. Soil Chemical Analysis—Advanced Course, 2nd Ed. Department of Soil Science, University of Wisconsin, Madison, WI.

James, R. V., and J. Rubin. 1986. Transport of chloride ion in a water-saturated soil exhibiting anion exclusion. Soil Sci. Soc. Am. J. 50(5):1142–1149.

Katou, H., B. E. Clothier, and S. R. Green. 1996. Anion transport involving competitive adsorption during transient water flow in an andisol. Soil Sci. Soc. Am. J. 60(5):1368–1375.

Ma, L., C. W. Lindau, C. Hongprayoon, W. Burhan, B. C. Jang, W. H. Patrick Jr., and H. M. Selim. 1999. Modeling urea, ammonium, and nitrate transport and transformations in flooded soil columns. Soil Sci. 164(2):123–132.

McBride, M. B. 1994. Environmental Chemistry of Soils. Oxford University Press, New York, NY.

Melamed, R., J. J. Jurinak, and L. M. Dudley. 1994. Anion exclusion-pore water velocity interaction affecting transport of bromine through an oxisol. Soil Sci. Soc. Am. J. 58(5):1405–1410.

Moore, D. M., and R. C. Reynolds Jr. 1997. Sample preparation techniques for clay minerals. *In*: X-ray Diffraction and the Identification and Analysis of Clay Minerals, 2nd Ed. Oxford University Press, New York, NY, pp. 211–213.

Nelson, D. W., and L. E. Sommers. 1982. Total carbon, organic carbon, and organic matter. *In*: Agronomy 9. A. L. Page, R. H. Miller, and D. R. Keeney (eds.). American Society of Agronomy, Madison, WI, pp. 539–579.

Nolan, B. T., and J. D. Stoner. 2000. Nutrients in ground waters of the conterminous United States, 1992–1995. Environ. Sci. Technol. 34(7):1156–1165.

Phillips, F. M., J. L. Mattick, T. A. Duval, D. Elmore, and P. W. Kubik. 1988. Chlorine 36 and tritium from nuclear weapons fallout as tracers for long-term liquid and vapor movement in desert soils. Water Res. Res. 24(11):1877–1891.

Porro, I., and P. J. Wierenga. 1993. Transient and steady-state solute transport through a large unsaturated soil column. Ground Water 31(2): 193–200.

Porro, I., P. J. Wierenga, and R. G. Hills. 1993. Solute transport through large uniform and layered soil columns. Water Res. Res. 29(4):1321–1330.

Ransom, M. D., J. M. Bigham, N. E. Smeck, and W. F. Jaynes. 1988. Transitional vermiculite-smectite phases in aqualfs of southeastern Ohio. Soil Sci. Soc. Am. J. 52:873–880.

Rhoades, J. D. 1982. Cation exchange capacity. *In*: Agronomy 9. A. L. Page, R. H. Miller, and D. R. Keeney (eds.). American Society of Agronomy, Madison, WI, pp. 149–157.

Rutledge, E. M., L. P. Wilding, and M. Elfield. 1967. Automated particle size separation by sedimentation. Soil Sci. Soc. Am. Proc. 31:287–288.

Ryan, M. C., G. R. Graham, and D. L. Rudolph. 2001. Contrasting nitrate adsorption in andisols of two coffee plantations in Costa Rica. J. Environ. Qual. 30(5):1848–1852.

Selim, H. M., and I. K. Iskandar. 1981. Modeling nitrogen transport and transformations in soils: Theoretical considerations. Soil Sci. 131(4): 233–241.

Skulka, M. K., and P. Cepuder. 2000. Anion exclusion during transport of chloride through soil columns. Trans. ASAE 43(6):1425–1430.

Smiles, D. E., and J. R. Philip. 1978. Solute transport during absorption of water by soil: Laboratory studies and their practical implications. Soil Sci. Soc. Am. J. 42:537–544.

Smith, S. J. and R. J. Davis. 1974. Relative movement of bromide and nitrate through soils. J. Environ. Qual. 3(2):152–155.

Sparks, D. L. 2003. Environmental Soil Chemistry, 2nd Ed. Academic Press, San Diego, CA.

Sposito, G. 1984. The Surface Chemistry of Soils. Oxford University Press, New York, NY.

Thomas, G. W., and A. R. Swaboda. 1970. Anion exclusion effects on chloride movement in soils. Soil Sci. 110(3):163–166.

Toner, C. V. IV, D. L. Sparks, and T. H. Carski. 1989. Anion exchange chemistry in middle Atlantic

soils: Charge properties and nitrate retention kinetics. Soil Sci. Soc. Am. J. 53(4):1061–1067.

US Department of Agriculture. 1954. Diagnosis and improvement of saline and alkaline soils. *In*: USDA Agricultural Handbook 60. L. A. Richards (ed.). US Government Printing Office, Washington, DC.

US Department of Agriculture, Economic Research Service. 1987. Farm drainage in the United States—History, status, and prospects. USDA Miscellaneous Publication 1455. US Department of Agriculture, Washington, DC.

US Environmental Protection Agency. 1979. Methods for Chemical Analysis of Water and Wastes. US Government Printing Office, Washington, DC.

US Geological Survey. 2001. Selected findings and current perspectives on urban and agricultural water quality by the National Water-Quality Assessment Program. US Geological Survey Fact Sheet 047-01. US Geological Survey, Reston, VA.

Wong, M. T. F., R. Huges, and D. L. Rowell. 1990. Retarded leaching of nitrate in acid soils from the tropics: Measurement of effective anion exchange capacity. J. Soil Sci. 41(4):655–663.

Wray, W. K. 1986. Measuring Engineering Properties of Soil. Prentice-Hall, Englewood Cliffs, NJ.

Zucker, L. A., and L. C. Brown. 1998. Agricultural drainage-water quality impacts and subsurface drainage studies in the Midwest. Ohio State University Extension Bulletin 871. Ohio State University, Columbus, OH.